 SDHM, vol.4, no.2, pp.77-93, 2008

A Generalized Technique for Fracture Analysis of 2-D Crack Problems Employing Singular Finite Elements

G.S. Palani[1], B. Dattaguru[2] and Nagesh R. Iyer[1]

Abstract: The objective of this paper is to present a generalized technique called as, numerically integrated Modified Virtual Crack Closure Integral (NI-MVCCI) technique for computation of strain energy release rate (SERR) for 2-D crack problems employing singular finite elements. NI-MVCCI technique is generalized one and the expressions for computing SERR are independent of the finite element employed. Stress intensity factor (SIF) can be computed using the relations between SERR and SIF depending on the assumption of plane stress/strain conditions. NI-MVCCI technique has been demonstrated for 8-noded Serendipity (regular & quarter-point) and 9-noded Lagrangian (regular & quarter-point) and 12-noded (regular & singular) isoparametric finite elements. Numerical studies on fracture analysis of mode-I and mode-II 2-D crack problems have been conducted employing these elements. SERR and SIF have been computed for these problems and found to be in good agreement with the respective infinite/finite plate solutions available in the literature. The appropriate Gauss numerical integration order to be employed for each of these elements, especially for the singular elements for accurate computation of SERR and SIF has been recommended based on the studies.

Keyword: Finite element method; Fracture mechanics; Numerical integration; Singular elements; Stress intensity factor

1 Introduction

The fracture behaviour of structural components under fatigue loading or during static overload can be estimated through linear elastic fracture mechanics (LEFM) principles, and SIF is the influencing design parameter. A detailed review of literature on fatigue and fracture behaviour of structural components was presented by Cotterell [2002] and Schijve [2003]. Using the finite element method (FEM) for basic stress analysis [Zienkiewicz and Taylor, (2000)], SIF can be computed through post-processing of finite element analysis (FEA) results [Liebowitz and Moyer, (1989)]. The techniques based on displacement extrapolation, strain energy release rate, virtual crack extension, modified virtual crack closure integral, equivalent domain integral and J-integral are generally preferred [Owen and Fawkes, (1982)], for computing SIF through post-processing of FEA results.

The major disadvantage in the extrapolation methods is that the accuracy in evaluating SIF depends on the accuracy of displacement and stress distribution in the vicinity of crack tips. As such, these methods are not suitable for use in conjunction with conventional finite elements and generally require stress analysis using singular elements only. The strain energy release rate and the virtual crack extension techniques require two runs of analysis for evaluating SERR. One of the popular post-processing techniques is MVCCI developed by Rybicki and Kanninen [1977] based on Irwin's crack closure integral (CCI) technique [Irwin, (1958)] with appropriate modifications for computation of SERR and SIF. Considering the merits and demerits of these techniques, it is observed that for LEFM problems, MVCCI technique in combination with FEM is an efficient tool for evaluating SERR from which SIF can be calculated. The advantage of MVCCI technique is its simplicity and also the ease with which individual mode SERR/SIF can be estimated in mixed-mode

[1] Structural Engineering Research Centre (SERC), CSIR Campus, Chennai, 600 113, India.
[2] Indian Institute of Science (IISc), Bangalore, 560 012, India

problems.

Rybicki and Kanninen [1977] expressed Irwin's CCI technique in a form consistent with the finite element (FE) formulation and evaluated SERR for mode I and II (G_I and G_{II}) in terms of nodal forces and displacements. Further, these computations can be carried out from a single FEA, as against from two analyses with crack lengths differing by an infinitesimally small crack length as conceived originally. Buchholz [1984] realized the element dependence of MVCCI equations and presented appropriate equations for 8-noded quadrilateral elements, but did not establish a formal procedure for deriving them. Badari Narayana and Dattaguru [1996] and Badari Narayana et al. [1990] presented the generalised MVCCI equations for conventional and singular quadrilateral elements for 2-D problems with cracks. Raju [1986] also derived MVCCI equations for 6-noded and 8-noded quarter-point singular elements. Young and Sun [1993] demonstrated the application of MVCCI technique to plate bending problems. Buchholz et al. [2001] and Dhondt et al. [2001] conducted fracture analysis to study the 3-D and mode coupling effects by employing MVCCI method.

For successful application of MVCCI technique, it is essential [1991] to derive element dependent MVCCI expressions for computation of SERR. The derivation of MVCCI expressions involves evaluation of constants used in the polynomial assumed to represent displacement and stress variation and evaluation of many integrals having complicated polynomial terms. This makes the derivation of MVCCI expressions a tedious exercise for higher order and singular 2-D and 3-D finite elements. However, the above problem can be simplified by employing numerically integrated approach that will also generalize the procedures. Palani et al. [2004] proposed numerically integrated MVCCI (NI-MVCCI) technique for 2-D crack problems. In this paper, this generalized technique has been proposed for 8-noded, 9-noded and 12-noded singular finite elements for computation of SERR and SIF for 2-D crack problems. One of the key features of the proposed NI-MVCCI technique is that it is general and is independent of the type of finite element employed. The efficacy of NI-MVCCI technique has been demonstrated for 8-noded Serendipity (regular & quarter-point), 9-noded Lagrangian (regular & quarter-point) and 12-noded (regular & singular) cubic isoparametric quadrilateral finite elements. For non-singular (regular) elements at crack tip NI-MVCCI technique generates the same results as MVCCI, but the advantage for higher order regular and singular elements is that complex expressions for MVCCI need not be derived. Numerical studies on fracture analysis of 2-D crack (mode I and II) problems have been conducted. Based on the studies, Gauss numerical integration rule to be employed for each of these elements for accurate computation of SERR and SIF has been recommended.

2 MVCCI Technique for 4-noded, 8-noded and 9-noded Quadrilateral Elements

Irwin [1958] proposed CCI technique for evaluation of SERR. CCI was derived using a fundamental concept that when crack extension takes place, the energy required to close this part of crack in a solid is same as the energy released during crack extension. The rate of change of this energy with crack extension is SERR, which is generally denoted as G. Fig. 1 shows a crack tip in an infinite isotropic media subjected to remote tensile loading causing mode I crack deformation. The normal stress distribution ahead of the crack tip is σ_{yy}. Let the crack of length, 'a' be extended by a small virtual increment of 'Δa'. The crack opening displacement (COD) behind the new crack tip is U_y (half of the total COD). The energy required to close the extended crack 'Δa' can be estimated as the work done by forces corresponding to the stress distribution, σ_{yy} on COD, U_y. This can be expressed as

$$W = \frac{1}{2}\int_{0}^{\Delta a} \sigma_{yy} U_y dx \tag{1}$$

The above CCI can be used to compute SERR as

$$G = \underset{\Delta a \to 0}{Lt} \frac{1}{2\Delta a}\int_{0}^{\Delta a} \sigma_{yy} U_y dx \tag{2}$$

Taking polar coordinate system $(r,\ \theta)$ with the origin at the crack tip in a 2-D domain and using Eq. (2), SERR for mode I and II cracks (G_I and G_{II}) can be expressed as

$$G_I = \underset{\Delta a \to 0}{Lt} \frac{1}{2\Delta a} \int_0^{\Delta a} \sigma_{yy}(r = x, \theta = 0) \\ U_y(r = \Delta a - x, \theta = \pi) dr \quad (3)$$

$$G_{II} = \underset{\Delta a \to 0}{Lt} \frac{1}{2\Delta a} \int_0^{\Delta a} \sigma_{xy}(r = x, \theta = 0) \\ U_x(r = \Delta a - x, \theta = \pi) dr \quad (4)$$

where σ_{yy} ($r = x$, θ=0) and σ_{xy} ($r = x$, θ = 0) are distribution of stresses ahead of the crack tip. U_x $(r = \Delta a - x,\ \theta = \pi)$ and U_y $(r = \Delta a - x,\ \theta = \pi)$ are the relative sliding and opening displacements between the crack faces and Δa is the virtual crack increment.

The problem is basically to evaluate the SERR which is represented as G = $(\partial U/\partial a)$. If one could conduct two stage FEA, SERR is obtained from the difference in the strain energies stored for the configurations corresponding to crack sizes 'a' and '$a + \Delta a$'. However, if 'Δa' is kept very small, one could use the stress distribution ahead of the crack tip (OA – represented using the local axis ξ as shown in Fig. 2 and COD behind the crack tip (OB - represented using the local axis ξ' as shown in Fig. 2 derived from a single FEA at crack length 'a' to evaluate MVCCI using Eqs. (3) and (4). Expressing these integrals in terms of nodal forces and displacements from FEA is the crux of MVCCI technique. Rybicki and Kanninen [1977] proposed FEA based MVCCI expressions for G_I and G_{II} for the constant strain triangles and 4-noded bilinear elements around the crack tip as follows:

$$G_I = \frac{1}{2\Delta a}[F_{y,j}(U_{y,(j-1)} - U_{y,(j-1)'})] \quad (5)$$

$$G_{II} = \frac{1}{2\Delta a}[F_{x,j}(U_{x,(j-1)} - U_{x,(j-1)'})] \quad (6)$$

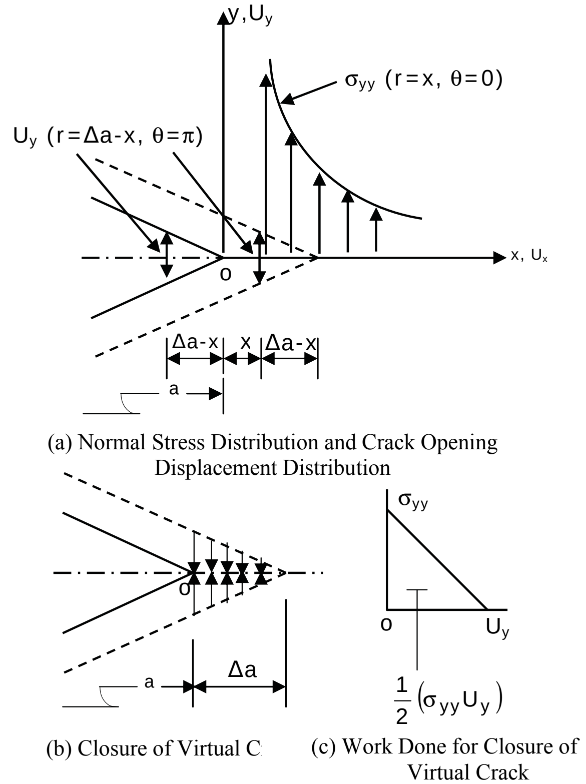

Figure 1: Schematic of Virtual Crack Extension (Mode I)

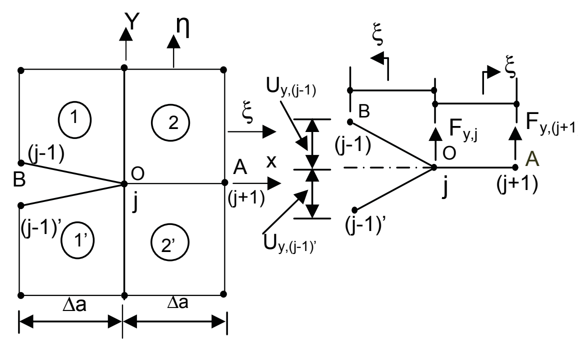

Figure 2: Typical FE Mesh of Crack Tip Region: 4-noded Elements

where $F_{y,j}$ and $F_{x,j}$ are the nodal forces at j in y- and x-directions computed for elements 1 and 2 as shown Fig. 2. The terms $U_{y,(j-1)}$ and $U_{y,(j-1)'}$ are nodal displacements at $(j-1)$ and $(j-1)'$ respectively in y-direction. The terms $U_{x,(j-1)}$ and $U_{x,(j-1)'}$ are nodal displacements at $(j-1)$ and

$(j-1)'$ respectively in x-direction. Each of the integrals for G_I and G_{II} is physically equivalent to the amount of work required to close the crack by an amount 'Δa'.

It is well-known that higher order elements can be used at the crack tip to get more accurate results with lesser computational effort. Consider the FE mesh near the crack tip as shown in Fig. 3, assembled with 8-noded quadrilateral elements with inside nodes at the mid-point of each side. SERR for mode I (G_I) can be evaluated by multiplying the stress distribution along OAB (local axis ξ) with the corresponding displacement distribution along OCD (local axis ξ') and integrating this product over Δa. This can be expressed [Badari Narayana, 1991] as

$$G_I = \frac{1}{2\Delta}\left[F_{y,j}\left(U_{y,(j-2)} - U_{y,(j-2)'}\right) + F_{y,(j+1)}\left(U_{y,(j-1)} - U_{y,(j-1)'}\right)\right] \quad (7)$$

where $F_{y,j'}$ $F_{y,(j+1)}$, and $F_{y,(j+2)}$ are the nodal forces acting at nodes j, $(j+1)$, and $(j+2)$ respectively.

Similarly, crack shearing displacement distribution is expressed in terms of nodal displacement $U_{x,(j-1)}$, $U_{x,(j-1)'}$, $U_{x,(j-2)}$ and $U_{x,(j-2)'}$. G_{II} can be expressed by replacing F_y by F_x and U_y by U_x in Eq. (7) as

$$G_{II} = \frac{1}{2\Delta}\left[F_{x,j}\left(U_{x,(j-2)} - U_{x,(j-2)'}\right) + F_{x,j+1}\left(U_{x,(j-1)} - U_{x,(j-1)'}\right)\right] \quad (8)$$

Eqs. (7) and (8) are also applicable for triangular elements obtained by collapsing the 8-noded quadrilateral elements at the crack tip. The forces at nodes j, $(j+1)$ and $(j+2)$ have to be obtained [Badari Narayana, 1991] from the contributions from all the triangular elements.

The quarter-point element (QPE) developed by Barsoum [1976] is widely used for fracture analysis of 2-D crack problems. QPE is a simple modification of the regular 8-noded element, which incorporates (1/$\sqrt{}$r) singularity at the crack tip. The required singularity is produced at the crack tip by moving midside nodes of an 8-noded element adjacent to the crack tip to the quarter-point position. It is ensured that such an element at the

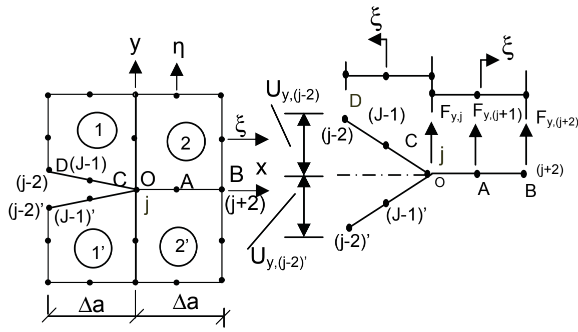

Figure 3: Typical FE Mesh of Crack Tip Region: 8-noded Regular Elements

crack tip satisfies inter-element compatibility with adjacent regular 8-noded elements. Referring to the rectangle in natural coordinate system, OCD corresponds to the crack face and OAB is the line of virtual crack extension. SERR for mode I crack (G_I) for this case can be expressed [Badari Narayana, 1991] as

$$G_I = \frac{1}{2\Delta a}\Big[\left(C_{11}F_{y,j} + C_{12}F_{y,(j+1)} + C_{13}F_{y,(j+2)}\right)\left(U_{y,(j-1)} - U_{y,(j-1)'}\right) + \left(C_{21}F_{y,j} + C_{22}F_{y,(j+1)} + C_{23}F_{y,(j+2)}\right)\left(U_{y,(j-2)} - U_{y,(j-2)'}\right)\Big] \quad (9)$$

where

$$C_{11} = \frac{33\pi}{2} - 52 \quad C_{12} = 17 - \frac{21\pi}{4}$$
$$C_{13} = \frac{21\pi}{2} - 32 \quad C_{21} = 14 - \frac{33\pi}{8}$$
$$C_{22} = \frac{21\pi}{16} - \frac{7}{2} \quad C_{23} = 8 - \frac{21\pi}{8}$$

In contrast to the regular 8-noded elements, the above expression for G_I for singular elements has cross terms involving all the force terms. The expression for G_{II} for 8-noded singular elements can be obtained by replacing F_y with F_x and U_y with

U_x, as

$$G_{II} = \frac{1}{2\Delta a}\Big[\big(C_{11}F_{x,j} + C_{12}F_{x,(j+1)} + C_{13}F_{x,(j+2)}\big) \big(U_{x,(j-1)} - U_{x,(j-1)'}\big) + \big(C_{21}F_{x,j} + C_{22}F_{x,(j+1)} + C_{23}F_{x,(j+2)}\big) \big(U_{x,(j-2)} - U_{x,(j-2)'}\big)\Big] \quad (10)$$

The expressions given by Eqs. (9) and (10) are also valid for triangular QPEs. For the case of triangular elements obtained by collapsing one side of the QPE at the crack tip, the evaluation of nodal forces $F_{x,j},\ F_{x,(j+1)}$ and $F_{x,(j+2)}$ has to be carried out by using the contributions from all the triangular elements.

3 Formulation of NI-MVCCI Technique

The derivation of element dependent MVCCI expressions for computing SERR for mode I and II cracks (G_I and G_{II}) as given by Eqs. (5) and (6) for 4-noded element, Eqs. (7) and (8) for 8-noded element and Eqs. (9) and (10) for 8-noded QPE involves evaluation of constants used in the polynomial assumed to represent displacement and stress variation and evaluation of many integrals having polynomial terms. As mentioned earlier, the derivation of MVCCI expressions becomes a tedious exercise for higher order 2-D (such as 12-noded singular) and 3-D (such as HEXA20 and HEXA27) finite elements. One of the main objectives of the current research work is to propose NI-MVCCI technique involving numerical techniques for computation of the constants and to evaluate CCI for G_I and G_{II} as given by Eqs. (3) and (4). NI-MVCCI is generalized technique and is independent of the type of finite element employed. Consider a typical FE mesh at the crack tip as shown in Fig. 4 The procedure for evaluating MVCCI for mode I and II cracks in 2-D problems using numerical techniques is explained. For mode I crack, SERR (G_I) can be evaluated by multiplying the stress distribution along OA (ahead of crack tip) with the corresponding COD distribution along OB (behind crack tip) and integrating this product over Δa.

For evaluation of SERR for mode I crack (G_I) the stress distribution on the crack extension line OA is expressed in terms of the nodal forces $F_{y,j}$, $F_{y,(j+1)}$, etc. acting at the nodes j, $(j+1)$, etc. respectively. COD distribution along OB is expressed in terms of the nodal values at j, $(j-1)$, $(j-1)'$, etc. SERR for mode I crack (G_I) is derived by evaluating the energy required to close the crack over a length Δa in terms of these nodal forces and displacements. The shape functions for elements 1 and 2 along OB can be obtained by substituting η=-1, in the respective element shape functions. Let these shape functions be N_i.

Let COD which is the difference between y displacement between the top and bottom faces be designated as U_y in the discussion in this section. Similarly crack shearing displacement be designated as U_x. COD distribution along OB can be expressed in terms of nodal displacements $\{(U_y)_i\}$ as

$$U_y = [N_i]\{(U_y)_i\} \quad i = 1,\ldots,n \quad (11)$$

where n is the number of nodes on the edge OA or OB of the element. Consistent with the isoparametric formulation, coordinate of any point $X(x,y)$ is given by

$$X = [N_i]\{(X)_i\} \quad i = 1,\ldots,n \quad (12)$$

where $\{(X)_i\}$ are the nodal coordinates. Eq. (12) thus provides the transformation between the global and natural coordinate system. Consistent with the element shape functions, COD variation along OB can be expressed as function of ξ' as

$$U_y(\xi') = a_0 + a_1\xi' + \ldots + a_{(n-1)}\xi'^{(n-1)} \quad (13)$$

where $U_y(\xi')$ is a polynomial of order (n-1). The constants a_0, a_1,…,$a_{(n-1)}$ can be evaluated by matching the displacement conditions at the nodes $j,(j-1),\ldots,(j-n+1)$ in element number 1. A set of simultaneous equations of order n is formed, which can be solved for obtaining the constants a_0, a_1,….,$a_{(n-1)}$.

Again referring to Fig. 4 and considering element number 2, stress (σ_y) distribution along OA can be expressed as a function of ξ

$$\sigma_y(\xi) = b_0 + b_1\xi + \ldots b_{(n-1)}\xi^{(n-1)} \quad (14)$$

where $\sigma_y(\xi)$ is a polynomial of order (n-1). The constants b_0, b_1,…,$b_{(n-1)}$ can be computed by matching the nodal forces with the derived consistent load vector from FE analysis. The nodal forces $F_{y,j}$, $F_{y,(j+1)}$,...,$F_{y,(j+n-1)}$ shown in Fig. 4 are the forces exerted at nodes $j,(j+1),\ldots,(j+n-1)$ by the structure below OA on the structure above OA. In FEA, these forces are obtained by adding the contributions of the forces at nodes $j,(j+1),\ldots,(j+n-1)$ from the elements on the edge above OA. These forces should be consistent with the stress distribution given in Eq. (14), which can be expressed as

$$F_i = \int_{\Delta a} [N_i]^T \sigma_y(\xi) dx \quad i = 1,\ldots,n \tag{15}$$

where N_i are the shape functions of the respective element obtained by substituting η=-1. By using the transformation between the global and natural coordinate system Eq. (12), the basis can be shifted from 'dx' to '$d\xi$'. The integrals given in Eq. (15) can be evaluated by numerical integration technique with suitable order. In the present study, Gauss integration technique has been employed with different integration rules.

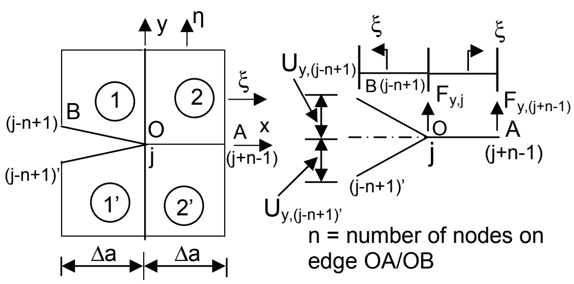

Figure 4: Typical FE Mesh of Crack Tip Region: NIMVCCI Technique

By substituting the expressions for COD and σ_y stress variations given by Eqs. (13) and (14) respectively in CCI Eq. (3), G_I can be expressed as

$$G_I = \underset{\Delta a \to 0}{Lt} \frac{1}{2\Delta a} \int_{\Delta a} \sigma_y(\xi) U_y(\xi') dx \tag{16}$$

Similarly, crack shearing displacement $U_x(\xi')$ and σ_{xy} distributions can be developed and G_{II} can be expressed as

$$G_{II} = \underset{\Delta a \to 0}{Lt} \frac{1}{2\Delta a} \int_{\Delta a} \sigma_{xy}(\xi) U_x(\xi') dx \tag{17}$$

The integrals given in Eqs. (16) and (17) can be performed by numerical integration technique. The numerical integration has to be carried out in two stages: One for evaluating the constants in σ_y (or σ_{xy}) distributions in terms of the nodal forces F_y (or F_x) in Eq. (15) and the second to evaluate the integral for G_I (or G_{II}) in Eq. (16) (or Eq. (17)). In the present study, Gauss integration technique has been employed for Eq. (16) with the same integration rule that is used for evaluating Eq. (15).

It can be observed from Eqs. (11) to (17), the proposed NI-MVCCI is a generalized technique and is independent of the type of element, except for assuming the expressions for displacement and stress variation (Eqs (13) and (14)). The order of polynomials for displacement and stress variation can be assumed to be consistent with the element shape functions along the edge η=-1. In the present study, NI-MVCCI technique is used to analyse crack problems with 8-noded (regular and quarter-point), 9-noded (regular and quarter-point) and 12-noded quadrilateral elements around the crack tip. MVCCI expressions for computing SERR for mode I and II cracks (G_I and G_{II}) using exact integration for 4-noded and 8-noded (regular & quarter-point) elements have been presented in Eqs (5)-(10). It may be noted that MVCCI expressions for 9-noded element will be same as that of 8-noded element. MVCCI expressions for 12-noded elements using exact integration have not been used to study crack problems in the literature. NI-MVCCI technique explained above can be easily implemented in any finite element code which has 8-noded (regular & quarter-point), 9-noded (regular & quarter-point) and 12-noded (regular & singular) quadrilateral isoparametric elements. However, some basic discussion on the polynomials to be selected will be required for implementation of NI-MVCCI technique for these elements. These basic expressions for each of these elements corresponding to Eqs. (11)-(17) are now presented:

8-noded and 9-noded (regular) quadrilateral elements

Shape functions (N_i) in Eqs. (11) and (15) along the edge OB as shown in Fig. 4 (for the edge OA replace ξ' by ξ) can be obtained by substituting η=-1 in 8-noded or 9-noded element shape functions.

$$N_i = 1/2(1+\xi'\xi'_i)\xi'\xi'_i \text{ for nodes with } \xi' = \pm 1 \tag{18a}$$

$$= 1/2(1-\xi'^2) \text{ for node with } \xi' = 0 \tag{18b}$$

Using the shape functions given in Eqs. (18a) and (18b), the transformation between global and natural coordinate system as given in Eq. (12) can be expressed as

$$x = -(\Delta a/2)(1+\xi') \tag{18c}$$

By substituting n=3 in Eq. (13), COD variation along OB can be assumed as

$$U_y(\xi') = a_0 + a_1\xi' + a_2\xi'^2 \tag{18d}$$

By substituting n=3 in Eq. (14), the stress variation along OA can be assumed as

$$\sigma_{yy}(\xi) = b_0 + b_1\xi + b_2\xi^2 \tag{18e}$$

Displacement and force conditions for evaluating the constants a_0, a_1, a_2 and b_0, b_1, b_2 can be expressed as

$$\begin{aligned} &U_y = 0 \text{ at } \xi' = -1;\\ &U_y = (U_{y,(j-1)} - U_{y,(j-1)'}) \text{ at } \xi' = 0;\\ &U_y = (U_{y,(j-2)} - U_{y,(j-2)'}) \text{ at } \xi' = 1; \end{aligned} \tag{18f}$$

$$\begin{aligned} &F_y = F_{y,j} \text{ at } \xi = -1;\\ &F_y = F_{y,(j+1)} \text{ at } \xi = 0;\\ &F_y = F_{y,(j+2)} \text{ at } \xi = 1; \end{aligned} \tag{18g}$$

Referring to Fig. 4, the relation between ξ' in element 1 and ξ in element 2 can be expressed as $\xi' = -\xi$.

8-noded [Barsoum, 1976] and 9-noded [Banks-Sills and Einav, 1987] QPE

Shape functions (N_i) in Eqs. (11) and (15) along the edge OB as shown in Fig. 4 (for the edge OA replace ξ' by ξ) can be obtained by substituting η=-1 in 8-noded QPE shape functions.

$$N_i = 1/2(1+\xi'\xi'_i)\xi'\xi'_i \text{ for node with } \xi' = \pm 1 \tag{19a}$$

$$= 1/2(1-\xi'^2) \text{ for node with } \xi' = 0 \tag{19b}$$

Using the shape functions given in Eqs. (19a) and (19b), the transformation between global and natural coordinate system as given in Eq. (12) can be expressed as

$$x = (\Delta a/4)(1+\xi')^2 \tag{19c}$$

By substituting n=3 in Eq. (13) and accounting for the quarter-point position of the midside node, COD variation along OB can be assumed as

$$U_y(\xi') = a_0 + a_1(1+\xi') + a_2(1+\xi')^2 \tag{19d}$$

In order to account for the singular stress conditions represented by QPE, the stress variation along OA can be assumed as

$$\sigma_{yy}(\xi) = b_0/(1+\xi) + b_1 + b_2(1+\xi) \tag{19e}$$

Displacement and force conditions for evaluating the constants a_0, a_1, a_2 and b_0, b_1, b_2 can be expressed as

$$\begin{aligned} &U_y = 0 \text{ at } \xi' = -1;\\ &U_y = (U_{y,(j-1)} - U_{y,(j-1)'}) \text{ at } \xi' = 0;\\ &U_y = (U_{y,(j-2)} - U_{y,(j-2)'}) \text{ at } \xi' = 1; \end{aligned} \tag{19f}$$

$$\begin{aligned} &F_y = F_{y,j} \text{ at } \xi = -1;\\ &F_y = F_{y,(j+1)} \text{ at } \xi = 0;\\ &F_y = F_{y,(j+2)} \text{ at } \xi = 1; \end{aligned} \tag{19g}$$

Referring to Fig. 4 and accounting for the quarter-point position of the midiside node, the relation between ξ' in element 1 and ξ in element 2 can be expressed as

$$(1+\xi)^2 + (1+\xi')^2 = 4 \tag{19h}$$

12-noded (regular) quadrilateral element

Shape functions (N_i) in Eqs. (11) and (15) along the edge OB as shown in Fig. 4 (for the edge OA replace ξ' by ξ) can be obtained by substituting η=-1 in 12-noded element shape functions.

$$N_i = 1/16(1+\xi'\xi_i')(-1+9\xi'^2) \quad \text{for nodes with } \xi' = \pm 1 \tag{20a}$$

$$N_i = 9/16(1+9\xi'\xi_i')(1-\xi'^2) \quad \text{for nodes with } \xi' = \pm 1/3 \tag{20b}$$

Using the shape functions given in Eqs. (20a) and (20b), the transformation between global and natural coordinate system as given in Eq. (12) can be expressed as

$$x = -(\Delta a/2)(1+\xi') \tag{20c}$$

By substituting n=4 in Eq. (13), COD the displacement variation along OB can be assumed as

$$U_y(\xi') = a_0 + a_1\xi' + a_2\xi'^2 + a_3\xi'^3 \tag{20d}$$

By substituting n=4 in Eq. (14), the stress variation along OA can be assumed as

$$\sigma_y(\xi) = b_0 + b_1\xi + b_2\xi^2 + b_3\xi^3 \tag{20e}$$

Displacement and force conditions for evaluating the constants a_0, a_1, a_2, a_3 and b_0, b_1, b_2, b_3 can be expressed as

$$\begin{aligned} &U_y = 0 \text{ at } \xi' = -1; \\ &U_y = (U_{y,(j-1)} - U_{y,(j-1)'}) \text{ at } \xi' = -1/3; \end{aligned} \tag{20f}$$

$$\begin{aligned} &U_y = (U_{y,(j-2)} - U_{y,(j-2)'}) \text{ at } \xi' = 1/3; \\ &U_y = (U_{y,(j-3)} - U_{y,(j-3)'}) \text{ at } \xi' = 1; \end{aligned} \tag{20g}$$

$$\begin{aligned} &F_y = F_{y,j} \text{ at } \xi = -1; \\ &F_y = F_{y,(j+1)} \text{ at } \xi = -1/3; \\ &F_y = F_{y,(j+2)} \text{ at } \xi = 1/3; \\ &F_y = F_{y,(j+3)} \text{ at } \xi = 1; \end{aligned} \tag{20h}$$

Referring to Fig. 4, the relation between ξ' in element 1 and ξ in element 2 can be expressed as $\xi' = -\xi$.

12-noded (singular) quadrilateral element [Pu etal., 1978]

Shape functions (N_i) in Eqs. (11) and (15) along the edge OB as shown in Fig. 4 (for the edge OA replace ξ' by ξ) can be obtained by substituting η=-1 in 12-noded element shape functions.

$$N_i = 1/16(1+\xi'\xi_i')(-1+9\xi'^2) \quad \text{for nodes with } \xi' = \pm 1 \tag{21a}$$

$$N_i = 9/16(1+9\xi'\xi_i')(1-\xi'^2) \quad \text{for nodes with } \xi' = \pm 1/3 \tag{21b}$$

Using the shape functions given in Eqs. (21a) and (21b), the transformation between global and natural coordinate system as given in Eq. (12) can be expressed as

$$x = (\Delta a/4)(1+\xi')^2 \tag{21c}$$

By substituting $n = 4$ in Eq. (13) and accounting for the position of the node adjacent to the crack tip for singularity, COD variation along OB can be assumed as

$$\begin{aligned} U_y(\xi') = a_0 + a_1(1+\xi') + a_2(1+\xi')^2 \\ + a_3(1+\xi')^3 \end{aligned} \tag{21d}$$

In order to account for the singular stress conditions for 12-noded element, the stress variation along OA can be assumed as

$$\sigma_{yy}(\xi) = b_0/(1+\xi) + b_1 + b_2(1+\xi) + b_3(1+\xi)^2 \tag{21e}$$

Displacement and force conditions for evaluating the constants a_0, a_1, a_2, a_3 and b_0, b_1, b_2, b_3 can be expressed as

$$\begin{aligned} &U_y = 0 \text{ at } \xi' = -1; \\ &U_y = (U_{y,(j-1)} - U_{y,(j-1)'}) \text{ at } \xi' = -1/3; \end{aligned} \tag{21f}$$

$$\begin{aligned} &U_y = (U_{y,(j-2)} - U_{y,(j-2)'}) \text{ at } \xi' = 1/3; \\ &U_y = (U_{y,(j-3)} - U_{y,(j-3)'}) \text{ at } \xi' = 1; \end{aligned} \tag{21g}$$

$$\begin{aligned} &F_y = F_{y,j} \text{ at } \xi = -1; \\ &F_y = F_{y,(j+1)} \text{ at } \xi = -1/3; \\ &F_y = F_{y,(j+2)} \text{ at } \xi = 1/3; \\ &F_y = F_{y,(j+3)} \text{ at } \xi = 1; \end{aligned} \tag{21h}$$

Referring to Fig. 4 and accounting for the position of the midside nodes at 1/9 and 4/9 positions, the relation between ξ' in element 1 and ξ in element 2 can be expressed as

$$(1+\xi)^2 + (1+\xi')^2 = 4 \tag{21i}$$

In the above detailed formulation of the generalized NI-MVCCI technique proposed in the current research work has been presented for computation of SERR and SIF for 2-D crack problems. As it can be observed, one of the key features of the proposed NI-MVCCI technique is that it is general and is independent of the type of finite element employed. The basic procedure will be the same for 3-D problems, if the displacement and stress distributions (Eqs. (13) and (14)) are assumed appropriately and the line integrals (Eqs. (16) to (17)) are replaced with area integrals. The application of NI-MVCCI technique has been demonstrated for 8-noded Serendipity (regular & quarter-point), 9-noded Lagrangian (regular & quarter-point) and 12-noded (regular & singular) cubic isoparametric quadrilateral finite elements in the following section.

4 Numerical Studies

In order to verify and validate NI-MVCCI technique presented above, fracture analysis of 2-D cracked plates (mode I and II) has been conducted by employing 8-noded (regular & QPE), 9-noded (regular & QPE) and 12-noded (regular & singular) finite elements. Static analysis of the plates has been conducted by using FEM. A number of numerical studies employing different mesh configurations have been conducted. The graded FE idealization of the plate as shown in Fig. 6 has been chosen for conducting the further studies based on the convergence check and comparison of the stress pattern at the crack tip. Fracture analysis has been conducted by employing NI-MVCCI technique for computing SERR and SIF. Gauss numerical integration technique with different integration rules has been employed for evaluating the integrals associated with NI-MVCCI technique. In all the example problems, plane strain conditions have been assumed at the crack tip to compute SIF by using SERR values obtained using NI-MVCCI technique.

Example-1: Rectangular Plate with Center Crack under Uniaxial Tension

A rectangular plate with center crack subjected to uniaxial tensile loading (mode I) as shown in Fig. 5(a) has been analysed to compute SERR and SIF at the crack tip. One quarter of the plate with symmetric boundary conditions has been idealized (refer Fig. 6 for mesh employing 9-noded element) using 8-noded, 9-noded and 12-noded finite elements. Table 1 presents SERR and SIF values obtained in the present study using 8-noded (regular & QPE), 9-noded (regular & QPE) and 12-noded elements employing different integration rules along with the results obtained by using MVCCI technique with exact integration and the reference solutions available in the literature [Rooke and Cartwright, 1976]. The variation of SIF with respect to $\Delta a/a$ and W/a is shown in Fig. 7

Example-2: Rectangular Plate with Edge Crack under Uniaxial Tension

A rectangular plate with an edge crack subjected to uniaxial tensile loading (mode I) as shown in Fig. 5(b) has been analysed to compute SERR and SIF at the crack tip. FE idealization as shown in Fig. 6 has been used in the studies, considering half symmetry, with appropriate changes for the boundary conditions. Table 2 presents SERR and SIF values obtained in the present study using 8-noded (regular & QPE), 9-noded (regular & QPE) and 12-noded (regular & singular) elements employing different integration rules along with the results obtained by using MVCCI technique and the reference solutions available in the literature [Rooke and Cartwright, 1976]. The variation of SIF values with respect to $\Delta a/a$ and W/a is shown in Fig. 8.

Example-3: Rectangular Plate with Center Crack under Shear Load

A rectangular plate with a center crack subjected to shear load (mode II) has been analysed to compute SERR and SIF at the crack tip. The plate geometry and attributes are the same as that of Example-1. FE idealization as shown in Fig. 6 has been used in the studies, considering quarter symmetry, with appropriate changes for the loading and boundary conditions. Table 3 presents SERR and SIF values obtained in the present study using 8-noded (regular & QPE), 9-noded (regular & QPE) and 12-noded (regular & singular) elements employing different integration rules along with the results obtained by using MVCCI technique and the analytical solutions for an infinite plate. The variation of SIF values with respect to $\Delta a/a$ and W/a is shown in Fig. 9.

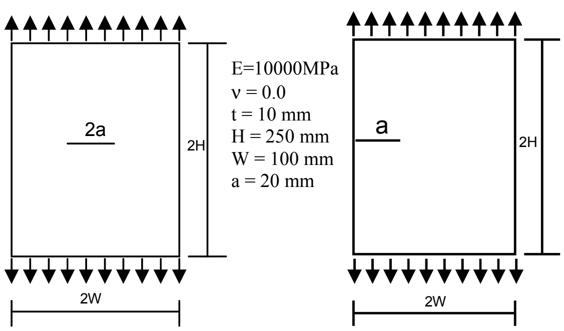

Figure 5: Rectangular Plate with (a) Center Crack (b) Edge Crack

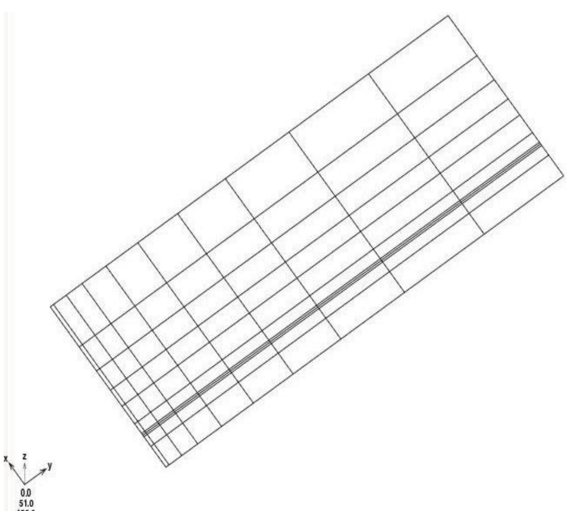

Figure 6: FE Idealization (9-noded element) of the Rectangular Plate (Quarter Symmetry)

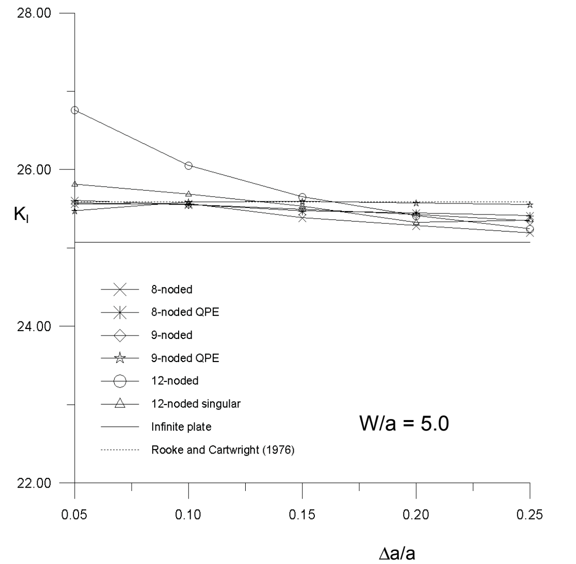

(a) Variation w.r.t. Δa/a

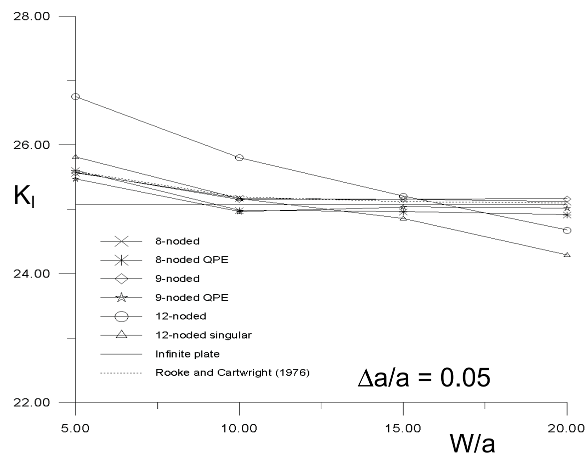

Figure 7: Variation of SIF for Rectangular Plate with Center Crack (Mode I)

4.1 Discussion of Results

It is observed from the studies (refer Figs. 8 to 10 and Tables 1 to 3) that SIF computed in the present study by employing NI-MVCCI technique along with 8-noded (regular & QPE), 9-noded (regular & QPE) and 12-noded (regular & singular) elements are generally in close agreement with the reference solutions for all the problems considered. In all the cases, except for singular elements (8-noded QPE, 9-noded QPE and

Table 1: SERR and SIF for Rectangular Plate with Center Crack under Uniaxial Tension (Comparison for different rules of Gauss integration for NI-MVCCI) ($\Delta a/a$=0.05 and W/a=5)

Gauss rule	8-noded element		8-noded QPE		9-noded element		9-noded QPE		12-noded element		12-noded Singular	
	G_I	K_I	G_I	K_I	G_I	K_I	G_I	K_I	G_I	K_I	G_I	K_I
2	0.10303	32.09787	0.04675	21.6224	0.09473	30.7777	0.06235	24.9695	0.32086	56.6447	13.75	370.81
3	0.06531	25.5559 (0.13)*	0.06612	25.7138	0.06539	25.5708 (0.08)*	0.06515	25.5235	0.39799	63.0866	0.06716	25.9161
4			0.06578	25.6480			0.06497	25.4897	0.06708	25.8998 (1.21)*	0.06660	25.8071
5			0.06567	25.6253			0.06491	25.4772			0.06661	25.8094
6			0.06561	25.6151			0.06488	25.4713			0.06661	25.8097
7			0.06559	25.6097			0.06486	25.4681			0.06661	25.8094
8			0.06557	25.6069			0.06485	25.4665			0.06661	25.8096
9			0.06556	25.6050			0.06485	25.4654			0.06661	25.8095
10			0.06556	25.6038 (0.05)*			0.06485	25.4647 (0.50)*			0.06661	25.8095 (0.86)*
MVCCI	0.06531	25.5559	0.06554	25.6005	0.06539	25.5708	0.06483	25.4627	0.06708	25.8998		

Analytical K_I: 25.59 [Rooke and Cartwright, 1976]; -% deviation from analytical K_I

Table 2: SERR and SIF for Rectangular Plate with Edge Crack under Uniaxial Tension (Comparison for different rules of Gauss integration for NI-MVCCI) ($\Delta a/a$=0.05 and W/a=5)

Gauss rule	8-noded element		8-noded QPE		9-noded element		9-noded QPE		12-noded element		12-noded Singular	
	G_I	K_I	G_I	K_I	G_I	K_I	G_I	K_I	G_I	K_I	G_I	K_I
2	0.20508	45.2856	0.07813	27.9509	0.17188	41.4578	0.07806	27.9399	0.64355	80.2219	17.75	421.307
3	0.11529	33.9546 (1.32)*	0.11724	34.2339	0.11577	34.0254 (1.12)*	0.11576	34.0235	0.15066	38.8151	0.11982	34.6157
4			0.11666	34.1548			0.11547	33.9805	0.11658	34.1443 (0.77)*	0.11648	34.1294
5			0.11646	34.1253			0.11536	33.9644			0.11651	34.1334
6			0.11636	34.1122			0.11531	33.9570			0.11652	34.1343
7			0.11632	34.1051			0.11528	33.9528			0.11651	34.1342
8			0.11629	34.1015			0.11527	33.9508			0.11652	34.1345
9			0.11628	34.0991			0.11526	33.9494			0.11652	34.1345
10			0.11626	34.0975 (0.92)*			0.11525	33.9485 (1.35)*			0.11652	34.1345 (0.80)*
MVCCI	0.11529	33.9546	0.11623	34.0932	0.11577	34.0254	0.11523	33.9459	0.11658	34.1443		

Analytical K_I: 34.41 [Rooke and Cartwright, 1976] - % deviation from analytical K_I

Table 3: SERR and SIF for Rectangular Plate with Center Crack under Shear Load (Comparison for different rules of Gauss integration for NI-MVCCI) ($\Delta a/a$=0.05 and W/a=20)

Gauss rule	8-noded element		8-noded QPE		9-noded element		9-noded QPE		12-noded element		12-noded Singular	
	G_{II}	K_{II}	G_{II}	K_{II}	G_{II}	K_{II}	G_{II}	K_{II}	G_{II}	K_{II}	G_{II}	K_{II}
2	0.10205	31.9454	0.07965	28.2225	0.09863	31.4059	0.05420	23.2807	0.31714	56.3151	2.00	141.421
3	0.06101	24.7001 (1.48)*	0.06108	24.7152	0.06206	24.9109 (0.63)*	0.06266	25.0315	0.08737	29.5591	0.01433	11.9722
4			0.06095	24.6894			0.06253	25.0066	0.06112	24.7225 (1.39)*	0.06118	24.7343
5			0.06089	24.6768			0.06248	24.9963			0.06117	24.7334
6			0.06087	24.6719			0.06246	24.9914			0.06116	24.7314
7			0.06086	24.6691			0.06244	24.9886			0.06116	24.7297
8			0.06085	24.6677			0.06244	24.9873			0.06115	24.7290
9			0.06085	24.6668			0.06243	24.9863			0.06115	24.7284
10			0.06084	24.6662 (1.61)*			0.06243	24.9857 (0.34)*			0.06115	24.7280 (1.36)*
MVCCI	0.06101	24.7001	0.06083	24.6645	0.06206	24.9109	0.06242	24.9839	0.06112	24.7225		

Analytical K_{II}: 25.07 -infinite plate soln. - % deviation from analytical K_I

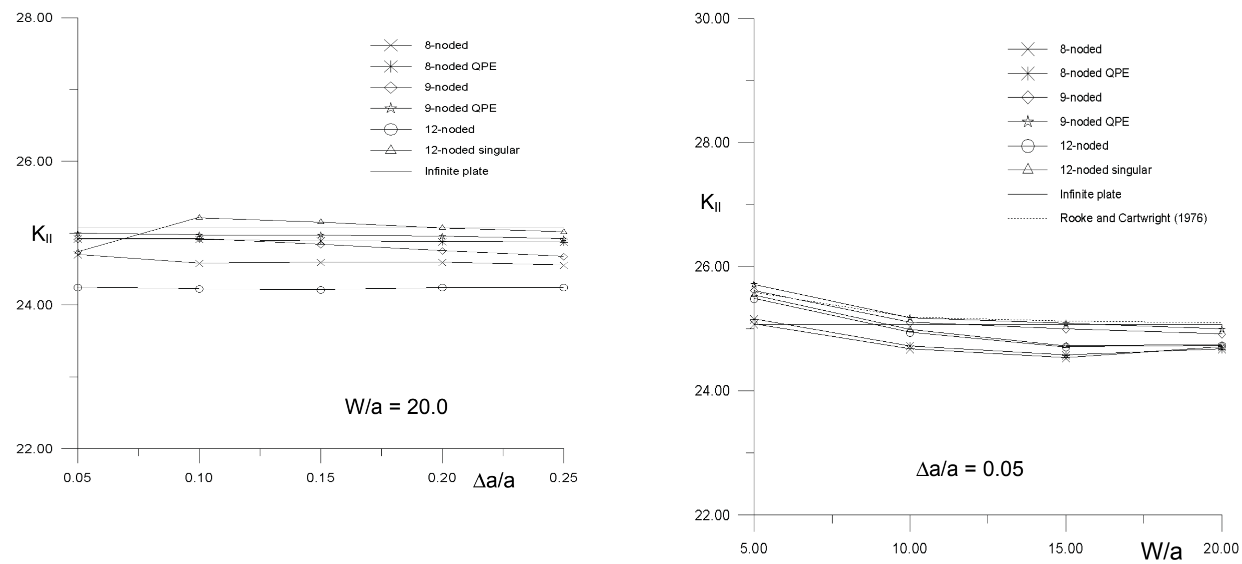

(a) Variation w.r.t. Δa/a (b) Variation w.r.t. W/a

Figure 9: Variation of SIF for Rectangular Plate with Center Crack (Mode II)

12-noded singular), NI-MVCCI technique serves the purpose of performing MVCCI integral exactly with appropriate rules of Gauss integration. For the regular elements as expected, NI-MVCCI technique using 3-point integration for 8-noded and 9-noded elements and 4-point integration for 12-noded element produced the same results as those obtained by using MVCCI technique. For the singular elements, 9-point integration along with 8-noded QPE, 9-noded QPE and 12-noded singular elements at the crack tip produced results within 1% of the reference solution. Lower order of integration is acceptable if one is willing to accept higher deviation with respect to the reference solution.

NI-MVCCI technique shows SIF estimations converge to the reference solution for 8-noded (regular & QPE), 9-noded (regular & QPE) and 12-noded (regular & singular) elements as $\Delta a/a \rightarrow 0$. It is interesting to note that 9-noded element performs well and converges faster than 8-noded and 12-noded elements to the reference solution as $\Delta a/a \rightarrow 0$. It can be observed from Figs. 8 to 10 that SIF obtained by employing 8-noded (regular & QPE) and 9-noded (regular & QPE) elements are in close agreement with the reference solution even for the highest $\Delta a/a$ ratio of 0.25 and is found not to vary significantly with $\Delta a/a$ ratio. SIF obtained by employing 8-noded and 9-noded (regular & QPE) elements converge to the analytical solution for an infinite plate as W/a is of the order of 20. The 9-noded Lagrangian element was not used much in the past, but the present study shows that it performs better than 8-noded and 12-noded Serendipity elements. This can be attributed to better stress recovery with 9-noded element.

For all the problems, elements with aspect ratio of 1.0 have been used at the crack tip. However, it was observed that this has resulted in deviation of SIF value obtained employing 12-noded (regular & singular) element from the reference solutions. After few trials, it was found that for this element, using an aspect ratio of 2.0 for the crack tip elements with the longer side perpendicular to the crack for mode I and along the crack for mode II problems, SIF values converge to the reference solution. This can be attributed to the errors in computing nodal stresses with 12-noded element that compensate each other.

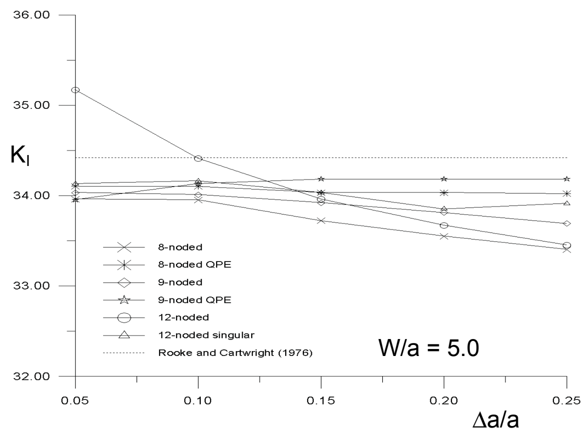

(a) Variation w.r.t. Δa/a

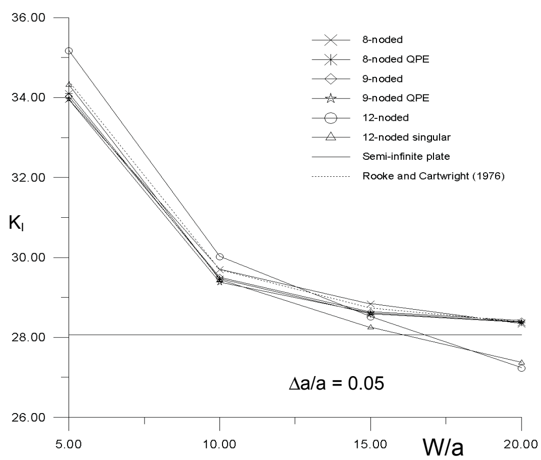

(b) Variation w.r.t. W/a

Figure 8: Variation of SIF for Rectangular Plate with Edge Crack (Mode I)

5 Summary and Conclusions

NI-MVCCI technique as a part of post-processing approach of FEA for computing SERR and SIF using for 2-D crack problems has been proposed. NI-MVCCI is a generalized technique and will remove the dependence of MVCCI equation on the type of finite elements employed in the basic stress analysis. The efficacy of NI-MVCCI technique has been demonstrated for 8-noded Serendipity (regular & QPE), 9-noded Lagrangian (regular & QPE) and 12-noded cubic (regular & singular) isoparametric finite elements. Based on the numerical studies conducted on cracked plates the following conclusions are drawn:

- NI-MVCCI is carefully formulated, since it involves two-way integration. The first integration is on stress distribution to express the constants in terms of nodal forces. The second integration estimates SERR.
- SIF computed in the present study by employing 8-noded (regular & QPE), 9-noded (regular & QPE) and 12-noded (regular & singular) elements generally compare well with the corresponding Reference solutions.
- For the regular elements as expected, NI-MVCCI technique using 3-point integration for 8-noded, 9-noded elements, 4-point integration for 12-noded element produced the same results as those obtained by using MVCCI technique.
- For 8-noded QPE, 9-noded QPE and 12-noded singular elements, NI-MVCCI technique using 9-point Gauss integration is recommended for evaluation of SERR and SIF as the evaluations are found to be within 1% accuracy for quarter-point elements.
- As $\Delta a/a \to 0$, results with 8-noded (regular & QPE) and 9-noded (regular & QPE) elements converge well to the reference solution.
- In general, SIF obtained employing 8-noded (regular & QPE) and 9-noded (regular & QPE) elements converge to the analytical solution for an infinite plate as W/a is of the order of 20.
- For 12-noded (regular & singular) element, using an aspect ratio of 2.0 for the crack tip elements with the longer side perpendicular to the crack for mode I and along the crack for mode II problems results in converging SIF values. This can be attributed to the errors in computing nodal stresses with 12-noded element that compensate each other.
- In general, 9-noded element performs well and converges faster than 8-noded and 12-noded elements to the reference solution as

$\Delta a/a \rightarrow 0$. The 9-noded Lagrangian element was not used much in the past, but the present study shows that it performs better than 8-noded and 12-noded Serendipity elements. This can be attributed to better stress recovery with 9-noded element.

- NI-MVCCI technique is found to be simple, powerful and effective technique for fracture analysis of 2-D crack problems. This technique can be easily implemented with any existing FEA software as a post-processing module.

Acknowledgement: Thanks are due to Shri J. Rajasankar and Shri A. Rama Chandra Murthy, Scientists, Structural Engineering Research Centre (SERC), Chennai, for the useful discussions and suggestions provided during the course of the investigations. This paper is being published with the kind permission of the Director, SERC, Chennai.

References

Badari Narayana, K. (1991): A general procedure for evaluation of crack closure integral in problems of fracture mechanics. *Ph. D. Thesis*, Indian Institute of Science, Bangalore, India,.

Badari Narayana, K.; Dattaguru, B. (1996): Certain aspects related to computation by modified crack closure integral. *Engg. Fract. Mech.*, 55:335-339.

Badari Narayana, K.; Dattaguru, B.; Ramamurthy, T.S.; Vijayakumar, K. (1990): Modified crack closure integral using 6-noded isoparametric quadrilateral singular element. Engg. Fract. Mech., 36:945-955.

Banks-Sills, L.; Einav, O. (1987): On singular, nine-noded, distorted, isoparametric elements in linear elastic fracture mechanics. Comput. Struct., 25:445-449.

Barsoum, R.S. (1976): On the use of isoparametric finite elements in linear fracture mechanics. Intl. Jl. Num. Meth. Engg., 10:25-37.

Buchholz, F.G. (1984): Improved formulae for the FE-calculation of the strain energy release rate by the modified crack closure integral method. *Proc. 4th World Congress and Exhibition in FEM*, 650-659.

Buchholz, F.G.; Chergui, A.; Richard, H.A. (2001): Computational fracture analysis by the MVCCI method regarding 3-D and mode coupling effects for different specimens and loading conditions. De Freitas M, Editor. *Proc. 6th Intl. Conf. Biaxial/Multiaxial Fatigue and Fracture,* Portugal, 991-998.

Cotterell, B. (2002): The past, present and future of fracture mechanics. *Engg. Fract. Mech.*, 69:533-553.

Dhondt, G.; Chergui, A.; Buchholz, F.G. (2001): Computational fracture analysis of different specimens regarding 3-D and mode coupling effects. *Engg. Fract. Mech.*, 68:383-401.

Irwin, G.R. (1958): Fracture. *Handbook Phys.*, 6:551-590.

Liebowitz, H., Moyer E.T. (1989): Finite element method in fracture mechanics. *Comput. Struct.*, 31:1-9.

Owen, D.R.J.; Fawkes, A.J. (1982): Engineering fracture mechanics: Numerical methods and applications, Swansea, UK: Pine Ridge Press Ltd.

Pu, S.L.; Hussian, M.A.; Lorensen, W.E. (1978): The collapsed cubic isoparametric element as a singular element for crack problems. *Intl. Jl. Num. Meth. Engg.*, 12:1727-1742.

Palani, G.S., Dattaguru, B. and Nagesh R. Iyer. (2004): Numerically Integrated Modified Virtual Crack Closure Integral technique for 2-D crack problems. *Intl. Jl. Struct. Engg. Mech.*, 18:731-744.

Rybicki, E.F.; Kanninen, M.F. (1977): A finite element calculation of stress intensity factors by a modified crack closure integral. *Engg. Fract. Mech.*, 9:931-938.

Raju, I.S. (1986): Simple formulas for strain energy release rate with singular order and simple finite elements. NASA-CR-178186.

Rooke, D.P.; Cartwright, D.T. (1976): Compendium of stress intensity factors. London: Her Majesty's Stationery Office.

Schijve, J. (2003): Fatigue of structures and materials in the 20th century and the state of the art. *Intl. Jl. Fatigue*, 25:679-702.

Young, M.J.; Sun, C.T. (1993): On the strain energy release rate for a cracked plate subject to out-of-plane bending moment. *Intl. Jl. Fract.*, 60:227-247.

Zienkiewicz, O.C.; Taylor, R.L. (2000): The Finite element method, Vol. I: The basis, Vol. II: Solid mechanics, Butterworth-Hieneman Ltd.